Supplemental Figure Legends

SFig. 1. *mdm10*Δ cells exhibit a delay in progression from G_1 to G_2. Wild-type (ISY001), *mdm10*Δ(ISY002) or rho^0 (ISY001-rho^0) yeast were grown in SC medium at 30^0C to mid-log phase (OD_{600} = 0.5 – 0.8). Cells were incubated with α-factor (10 μM) for 2.5 hrs to induce arrest in G_1 phase. Thereafter, they were washed with pheromone-free SC medium and incubated at 30°C. At various times min after release from pheromone-induced G_1 arrest, cells were fixed, stained with propidium iodide and analyzed for DNA content by flow cytometry. The percentage of total dividing cells in G_2 phase, as a function of time after release from pheromone-induced G_1 arrest, is shown. The basis for the reduced rate of progression of *mdm10*Δ cells from G_1 to G_2 is not clear. However, rho^0 cells, which have no mtDNA and severe defects in mitochondrial respiratory activity, progress from G_1 to G_2 phase at rates similar to that of wild-type cells. Thus, the reduced rate of cell cycle progression observed in *mdm10*Δ cells does not appear to be linked to mitochondrial respiration or dependent upon mtDNA.

SFig. 2. *mdm10*Δ cells exhibit a delay anaphase entry and mitotic exit. A) A wild-type strain (BY4741) and an *mdm10*Δ mutant strain (ISY002) were synchronized as for Fig. S1 and grown at 30°C. Aliquots were removed from cultures at the time indicated. Levels of Clb2p in synchronized cell cultures were determined by Western blot analysis using a polyclonal anti-Clb2p antibody. Hxk1p was used as a loading control. B) Wild-type (LGY020; black line) and *mdm10*Δ (LGY021; grey line) cells expressing plasmid-borne mCherry-tagged tubulin were synchronized and aliquots were removed from cultures at the times indicated, fixed and visualized by fluorescence microscopy. The number of cells with spindles > 4 μm in length was determined as a function of time after release from pheromone-induced G_1 arrest. Spindle assembly and disassembly are also delayed in *mdm10*Δ compared to wild type cells. We detect the maximum number of anaphase spindles, spindles that are 4-7 μm in length, within 60 min after release of wild-type cells from pheromone-induced G_1 arrest, and spindle disassembly 100 min after release from G_1 arrest. The kinetics of anaphase spindle assembly and disassembly in these synchronized wild-type cells are similar to those reported previously [7]. In contrast, deletion of *MDM10* results in a 25 min delay in spindle assembly and a 35 min delay in spindle disassembly. Accounting for the delay in anaphase onset, *mdm10*Δ cells exhibit a 10 min delay in mitotic exit. The delay in early anaphase and mitotic exit observed in *mdm10*Δ is similar to the delay in G_1 to G_2 phase progression. C) Quantitation of the timecourse for formation of second buds in multibudded *mdm10*Δ cells.

SFig. 3. *mdm10*Δ cells do not exhibit defects in septation. A) *cbk1*Δ and *mdm10*Δcells (ISY007 and ISY002) were grown to mid-log phase, fixed and incubated with zymolyase. Phase contrast images of *cbk1*Δ and *mdm10*Δ cells before and after cell wall digestion are shown. B) The number of multibudded cells in *cbk1*Δ and *mdm10*Δ cells before and after treatment with zymolyase. Error bars show standard deviations from n>800 measurements. Cell wall digestion dissociates multibudded cells with failed septum degradation (e.g. *cbk1Δ* cells) but has only a limited effect on multibudded cells produced by contractile ring defects. In contrast, similar treatment produced only a slight decrease in the number of cells in multibudded clumps of *mdm10*Δ cells. Thus, the multibudded phenotype in *mdm10Δ* cells is not due to a septation defect.

SFig. 4. Deletion of *MDM10* has no effect on spindle alignment or nucleolar segregation. A) Spindle and DNA were visualized in wild-type (BY4741) and *mdm10*Δ (Open Biosystems 398) by indirect immunofluorescence using antibodies that recognize tubulin and DAPI staining. Alignment of spindles ≥ 4 μm was assessed in wild-type cells 60 min after release from pheromone induced G1 arrest, and in *mdm10*Δ cells 120 min after release from G1 arrest. Spindles were scored as aligned if they were parallel to the mother-bud axis and any detectable bend in the spindle was <30° from mother-bud axis. In wild-type and *mdm10*Δ cells, 69.2% and 76.5% of the spindles examined exhibited proper alignment and orientation (n>100). B) For analysis of segregation of nucleolar material, mid-log phase wild-type cells (BY4741) and *mdm10*Δ cells (Open Biosystems 398) were fixed and stained for Nop1p, a nucleolar protein, by indirect immunofluorescence, and for DNA using DAPI. Analysis was restricted to cells in which DAPI-stained nuclear DNA masses were fully separated. DNA masses and Nop1p-stained nucleolus were fully separated in 96% of wild-type cells analyzed, and in 100% of *mdm10*Δ cells examined (n>50). Cell outlines are shown in white. Bar: 1 μm.

Fig. S5. Sli15p exhibits normal localization to the spindle apparatus in *mdm10*Δ cells. A) Wild-type (LGY022) and *mdm10*Δ (LGY023) Sli15p-GFP (green) and mCherry-tagged tubulin (red) were grown to mid-log phase, and fixed as for Fig. 1, in wild-type (top) and *mdm10*Δ (lower) cells. The images shown are 2-D projections from reconstructed 3-D volumes. Cell outlines are shown in white. Bar, 1 μm. B). Quantitation of Sli15p localization as a function of spindle length in wild-type and *mdm10*Δ cells. Error bars show standard error of the mean (n>200).

SFig. 6: Hyperactivation of the MEN suppresses the delay in mitotic exit observed in *mdm10*Δ cells. Wild-type (ISY001), *mdm10*Δ (ISY002) and *mdm10*Δ *bub2*Δ (ISY029) cells were synchronized with pheromone as for Fig. 2. Aliquots were removed from cultures at the times indicated and levels of Clb2p were determined by Western blot analysis using a polyclonal anti-Clb2p antibody. Hxk1p was used as a loading control. Hyperactivation of the MEN in *mdm10*Δ cells by-passes the subtle delay in mitotic cyclin degradation.

Supplemental Fig 1

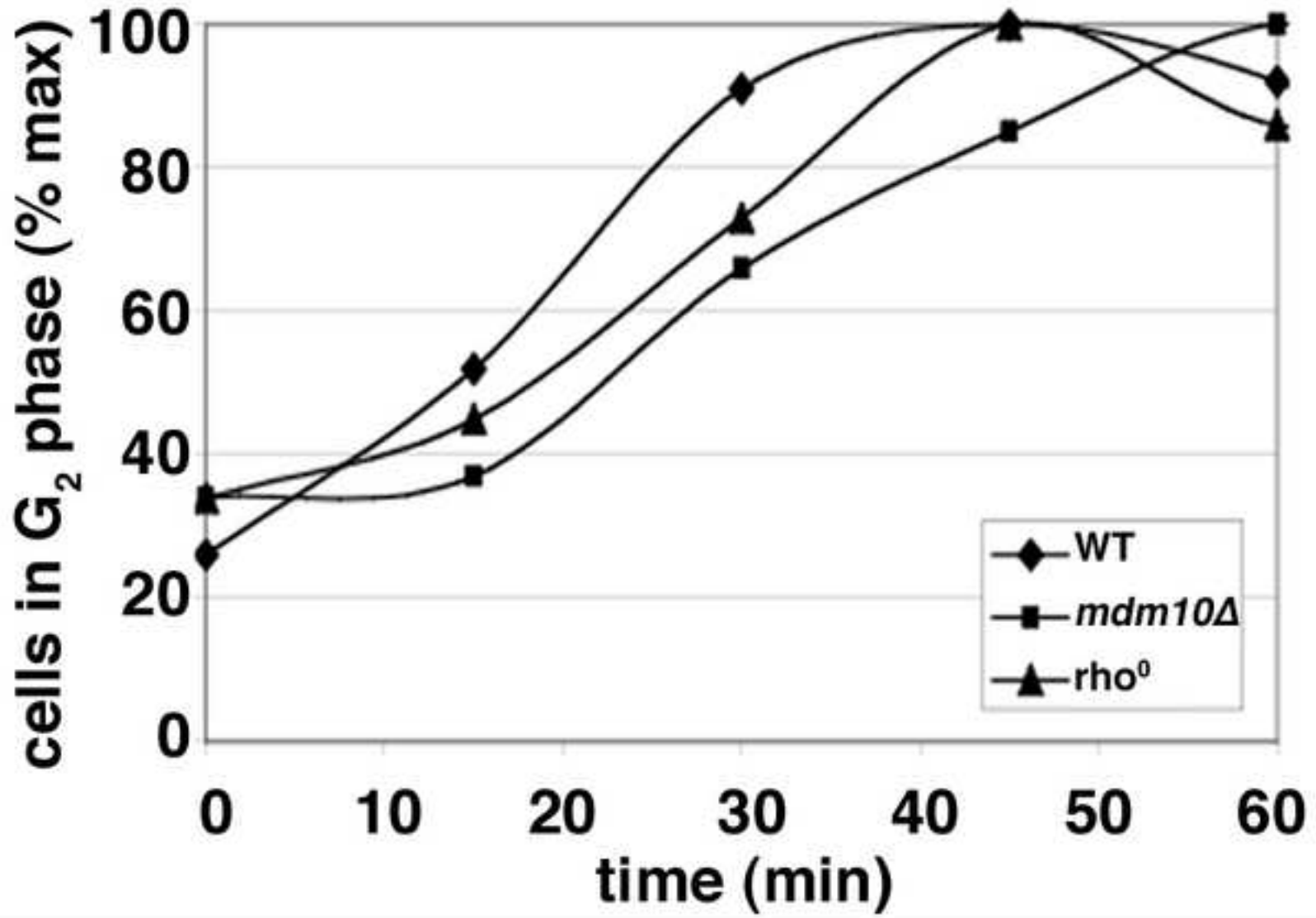

Supplemental Fig 2

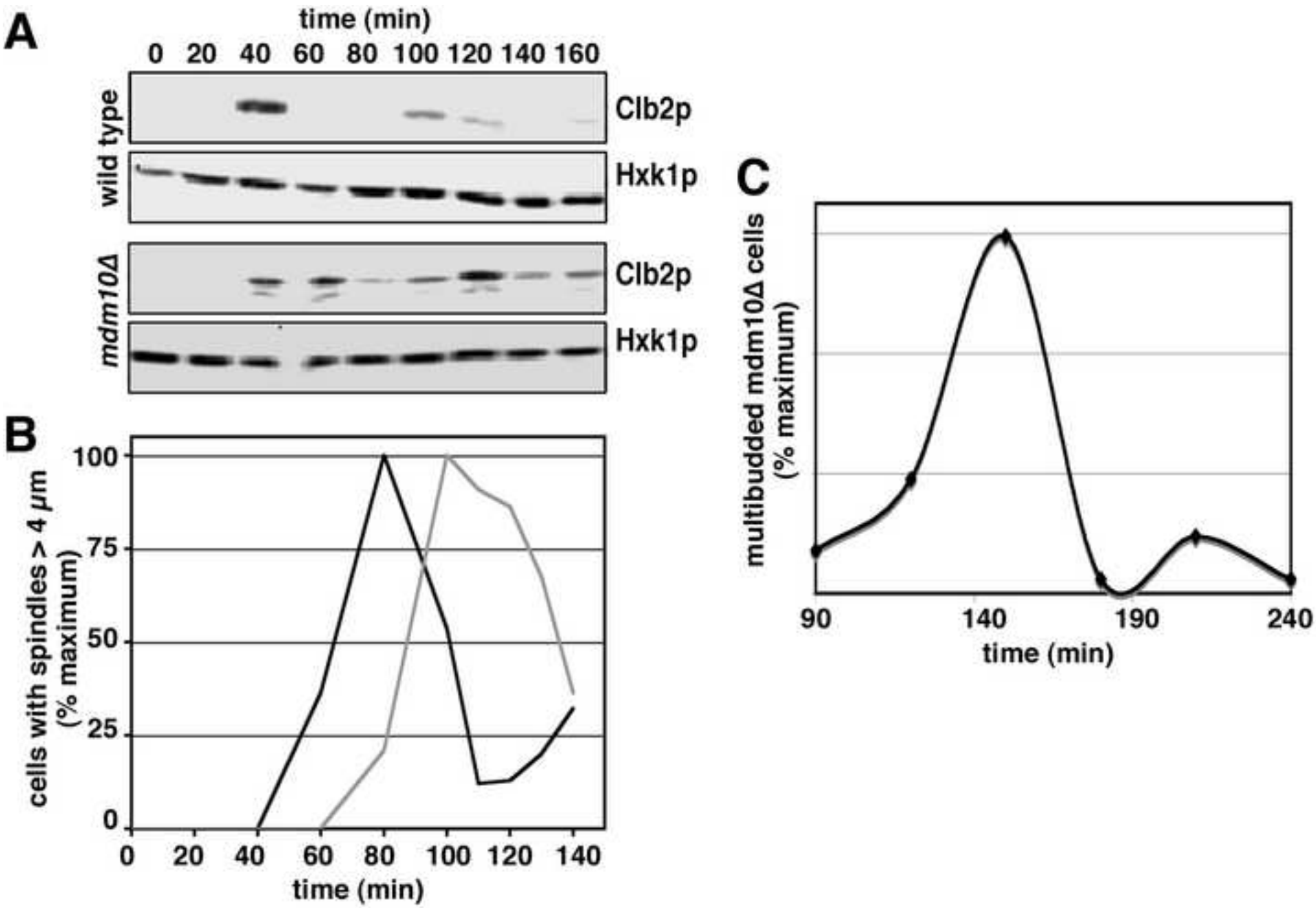

Supplemental Fig 3

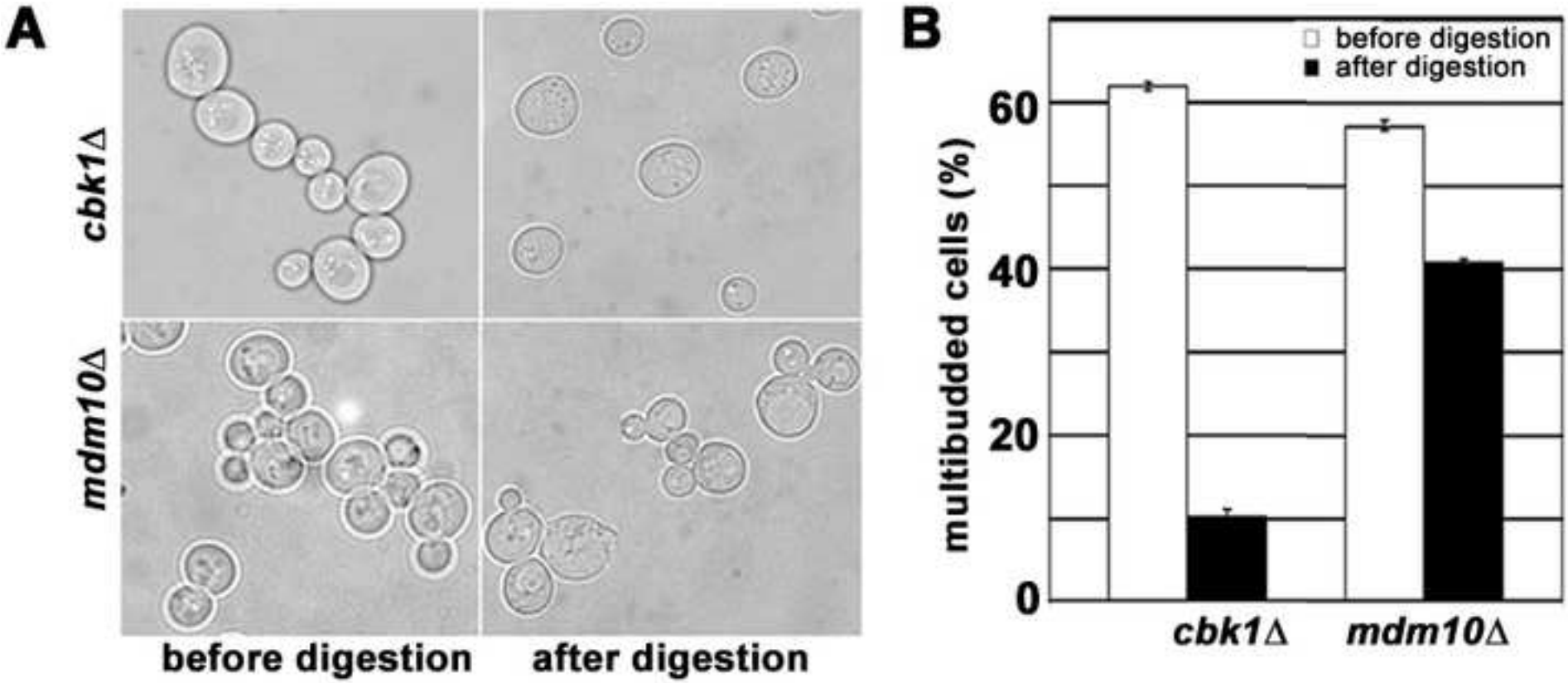

Supplemental Fig 4

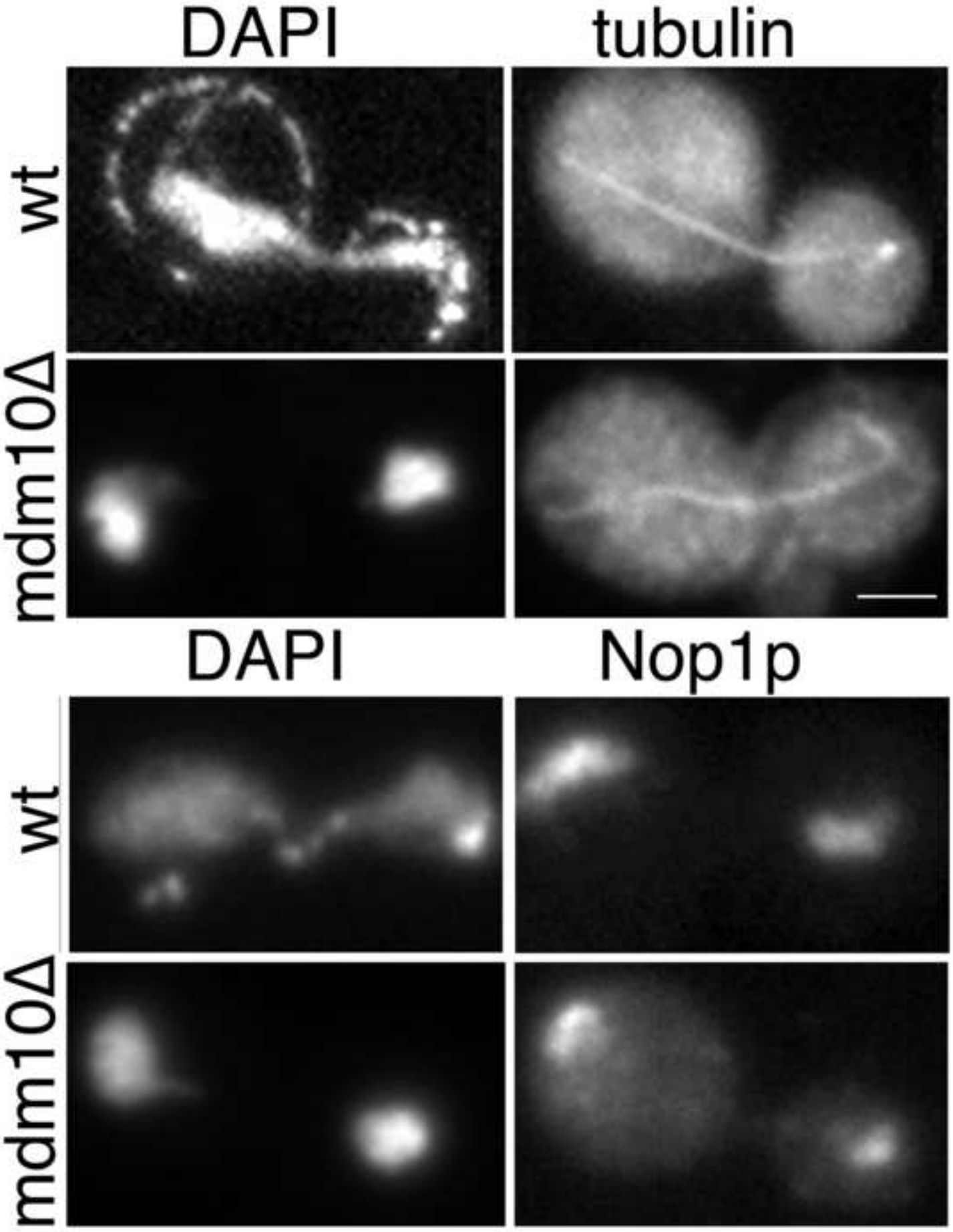

Supplemental Fig 5

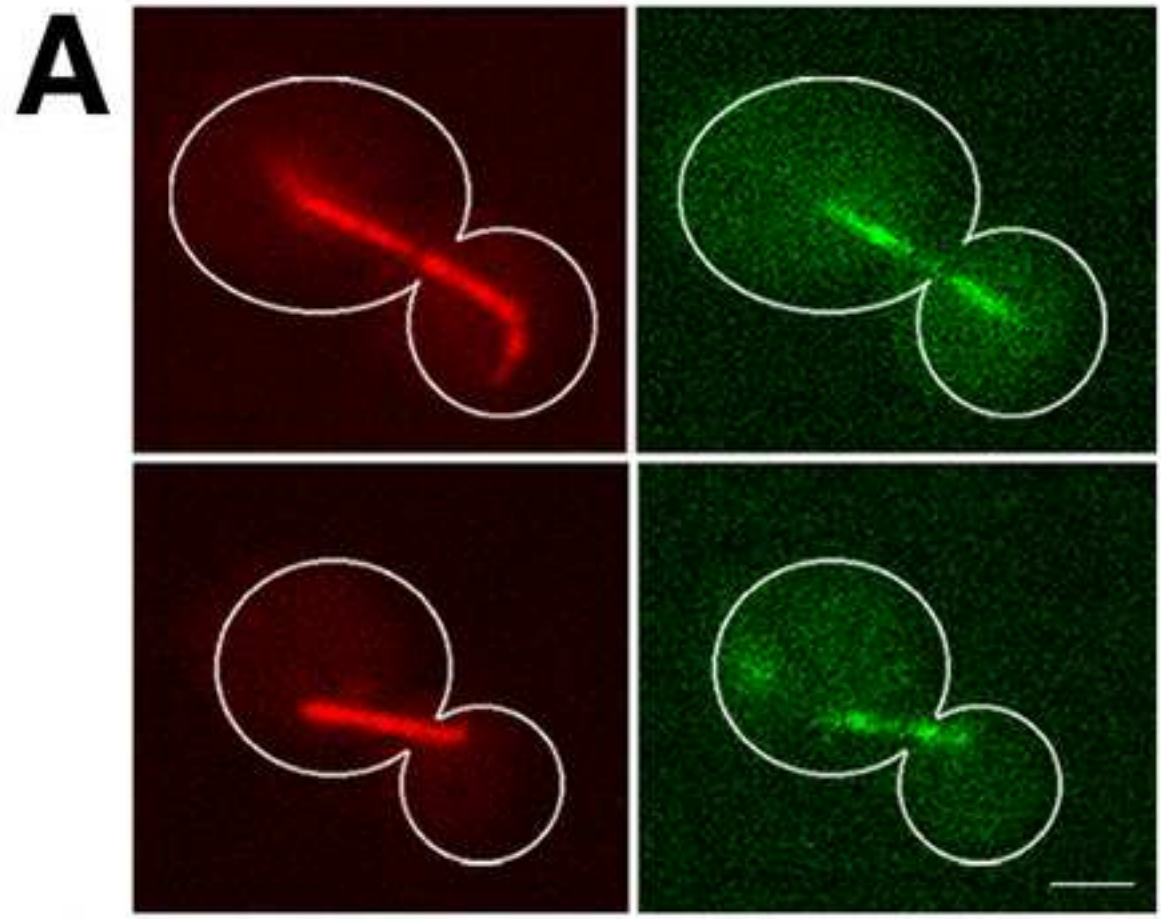

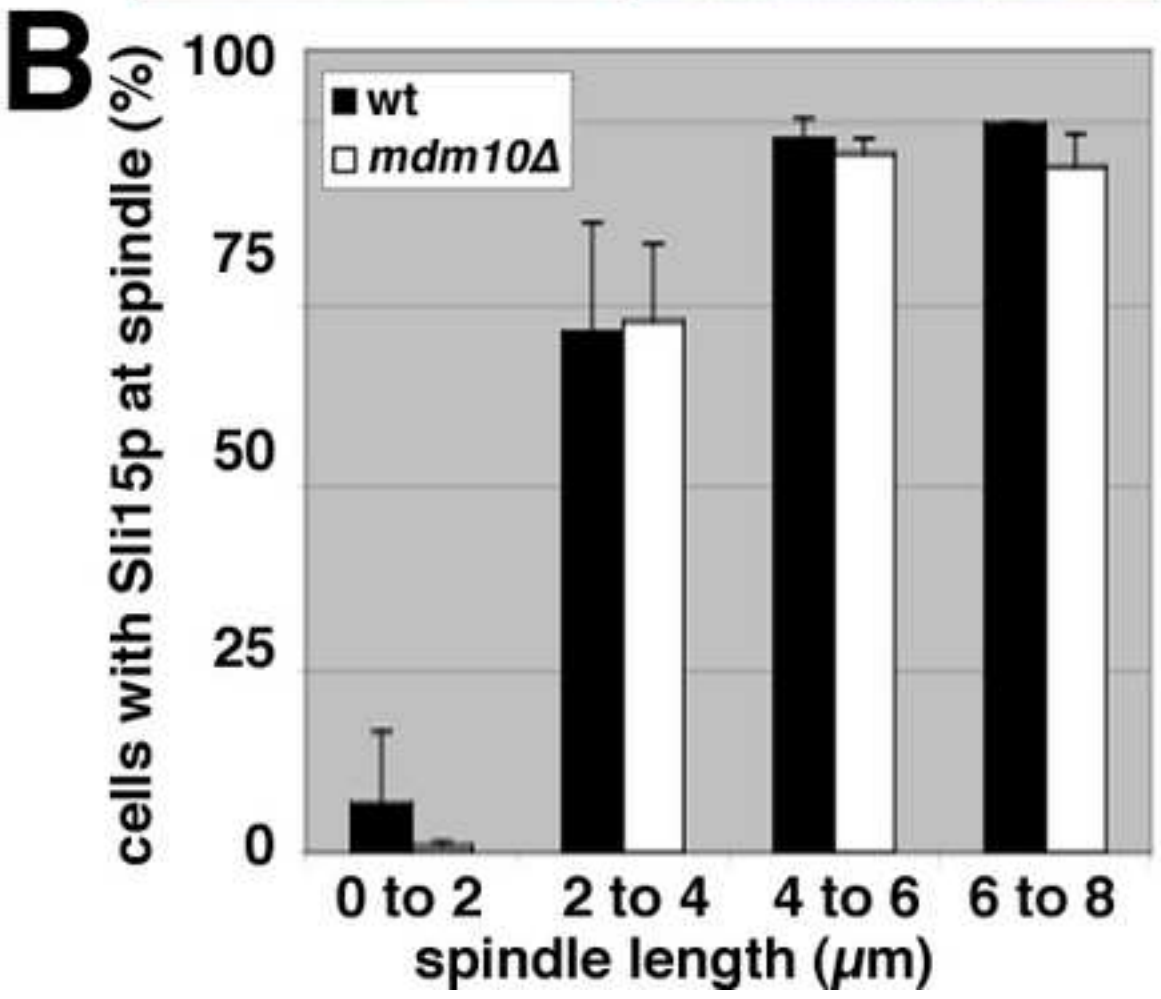

Supplemental Fig 6